

COMITATO NAZIONALE PER L'ENERGIA NUCLEARE
Istituto Nazionale di Frascati

LNF - 68/38
27 Giugno 1968

M. Greco, A. Tenore and A. Verganelakis : VIRTUAL PROTON
COMPTON EFFECT AND THE ELECTRON (MUON). - PROTON
BREMSSTRAHLUNG AS A TEST OF QUANTUM ELECTRODYN-
AMICS.

Laboratori Nazionali di Frascati del CNEN
Servizio Documentazione

LNF-68/38

Nota interna: n. 405
27 Giugno 1968

M. Greco, A. Tenore and A. Verganelakis^(x): VIRTUAL PROTON COMPTON EFFECT AND THE ELECTRON (MUON)-PROTON BREMSSTRAHLUNG AS A TEST OF QUANTUM ELECTRODYNAMICS.

ABSTRACT -

The virtual proton Compton Effect is studied in the approximation of a single virtual proton and a 3-3 resonance. The computation of the latter intermediate state is carried out in the framework of isobaric formalism.

The contribution to the measurements of the wide angle bremsstrahlung, arising from the virtual proton Compton terms, is given explicitly. It is shown that these contributions depend strongly on the kinematical configuration of the experiments and may change appreciably the results of pure QED in the critical region where the intermediate electron or muon is far off its mass shell. The numerical results suggest that the exponential form factor is a more reasonable one, to describe the behaviour of the γNN^* vertex form factor. In addition it is pointed out

(x) - Istituto di Fisica dell'Università di Roma and Laboratori del CNEN, Frascati (Italy). - On leave from NRC "Democritos", Athens, Greece.

2.

that proton polarization measurements in the wide-angle bremsstrahlung and large angle pair production experiments, provide one with a new important source of information about the contribution of the virtual proton Compton effect to these processes. Polarized cross sections are explicitly calculated.

1 - INTRODUCTION -

As it is well known there are two complementary classes of experiments for studying the limits of validity of QED. There are the low-energy, high-accuracy atomic measurements (Hydrogen Hyperfine structure; Lamb shift, etc.) and high-energy, lower-accuracy measurements, (Large Angle pair production, Wide-Angle bremsstrahlung etc.). The former class has been well studied in the past, while only recently, with the improvement of the experimental techniques, the latter has begun to be explored.

In fact in the last five years several high-energy experiments have been performed⁽¹⁾ or are now under way, which are designed to study the behaviour of amplitudes, in which an intermediate electron or muon is far off the mass shell.

Often the theoretical interpretation of these experiments goes as follows: first it is supposed that contributions to the measurements that are not interesting from the stand point of testing QED, are known exactly. Secondly one calculates the amplitude of the QED process in conventional perturbation theory. Then one compares the ratio of the experimental results to theoretical predictions, seeing to what extent various conjectured changes in the Green's function, in particular the electron (muon) propagator⁽²⁾, are limited, or possibly required, by experiment.

In the case of the electron (muon) - proton wide-angle bremsstrahlung (WAB):

$$(I. 1) \quad e(\mu) + p \longrightarrow e(\mu) + p + \gamma,$$

the first order Feynman diagrams are shown in Fig. 1: (a) and (b) are the so called Bethe-Heitler (BH) diagrams and (c) is the virtual proton Compton (VPC) diagram. The contribution to the measurements arising from diagram (c) is the uninteresting one for testing QED. However, it is desirable to know exactly this contribution, in order to avoid as far as it is possible the introduction of uncertainties into the interpretation of the experimental data. In principle the interference of diagram (c) with the BH

terms can be eliminated by using as probe particles both e^+ and e^- (μ^+ and μ^-) under exactly symmetrical kinematical configurations^(x), but what always remains is the modulus of the amplitude of this diagram.

So far only the contributions arising from the single nucleon intermediate state of the diagram 1(c) have been evaluated⁽⁴⁾. Previous attempts to estimate the contribution of the $N^*(1238)$ resonance intermediate state suffered from many poorly justified approximations⁽⁵⁾.

We have tried to improve the accuracy to which the contribution of the VPC amplitude to the WAB is known, by approximating the blob of the diagram of Fig. 1(c) by the contributions of a single virtual proton and a 3-3 resonance. The computation of the latter intermediate state contribution has been carried out in the framework of isobaric formalism, under the assumption that the 3-3 resonance is an elementary particle described by a Rarita-Schwinger spin 3/2 field. In a previous paper⁽⁶⁾ we have reported explicit results showing that the importance of the VPC contribution to the WAB depends on the kinematical configuration of the experiment, and may change appreciably the results expected from pure QED, at critical points at which the intermediate electron or muon is far off its mass shell. Also we have suggested that the study of polarization phenomena in the WAB and large-angle pair production experiments, provides us with a new source of information and helps us to gain a better understanding of the VPC effects, offering a test of the reliability of our calculations.

In view of the fact that in designing future experiments concerning the process (1), either for testing QED or for studying the VPC effect, more information will be needed, we report here an extensive description of the VPC amplitude as well as of various measurable quantities related to the WAB process. Direct application of the results given below is found also in the π^0 electroproduction experiments, in various sum rules, etc. On the other hand by making use of the substitution rule it is easy to extend these results to the photoproduction of large angle pairs.

The program of the present paper is as follows: in section II the form of the matrix element of the WAB process is given. Section III deals with the differential cross section, unpolarized target; differential cross section, polarized target; and polarization of the recoil proton. In section IV the VPC amplitude in the approximation of a single nucleon and 3-3 resonance intermediate state is given explicitly. In section V our numerical calculations and results are reported and in section VI a discussion of our results is presented. In the appendix we give the notation used and useful formulas.

(x) - An analogous situation is found in the photoproduction of large-angle pairs in which the interference between the BH and VPC amplitude can be avoided in a symmetrical arrangement, where charges and polarizations of the final leptons are not observed⁽³⁾.

II. FORM OF THE MATRIX ELEMENT -

We begin by stating our notational conventions. We adopt the Lorentz signature (+, -, -, -) for $g^{\mu\nu}$, the alternating tensor $\epsilon_{\mu\nu\rho\sigma}$ with $\epsilon_{0123} = - \epsilon^{0123} = +1$ and the four-vector p with components $p^\mu = (E, \vec{p})$, $\mu = 0, 1, 2, 3$. We use the notation $\tilde{p} = p^\mu \gamma_\mu$. For Dirac matrices and spinor normalization we use the same conventions as Bjorken and Drell⁽⁷⁾.

Let us adopt the particle labels indicated in Fig. 1 where ϵ is the polarization four-vector of the real photon. The amplitude F is defined by:

$$(II. 1) \quad S = 1 + i(2\pi)^4 \delta^4(p_1 + p_2 - p_3 - p_4 - k) \left(\frac{m^2}{E_1 E_3}\right)^{1/2} \left(\frac{M^2}{E_2 E_4}\right)^{1/2} \left(\frac{1}{2k_0}\right)^{1/2} F.$$

We are using natural units ($\hbar = c = 1$). F may be written as the sum of two amplitudes.

$$(II. 2) \quad F = F^{BH} + F^{VPC}$$

where in F^{BH} and F^{VPC} are included the amplitudes of BH diagrams and of VPC diagrams respectively.

In conventional perturbation theory the F^{BH} has the form

$$(II. 3) \quad F^{BH} = c_1 \bar{u}(p_3) \epsilon'^\rho M'_{\rho\lambda} \epsilon^\lambda u(p_1)$$

where ϵ is the real photon polarization, c_1 is a constant, and

$$(II. 4) \quad \epsilon'_\rho = \frac{1}{q^2} u(p_4) \Gamma_\rho u(p_2),$$

$$(II. 5) \quad \Gamma^\rho = e \left\{ F_1(q^2) \gamma^\rho + \frac{i\mu}{2M} F_2(q^2) \sigma^{\rho n} q_n \right\},$$

with $F_1(q^2)$ and $F_2(q^2)$ the Dirac and Pauli proton form factors respectively, normalized to $F_1(0) = F_2(0) = 1$, μ is the anomalous magnetic moment in units of the nuclear magneton, and finally

$$(II. 6) \quad M'_{\rho\lambda} = \left(\frac{p_3 \lambda}{p_3 \cdot k} - \frac{p_1 \lambda}{p_1 \cdot k} \right) \gamma_\rho + \left(\frac{\gamma_\rho \tilde{k} \gamma_\lambda}{2p_1 \cdot k} + \frac{\gamma_\lambda \tilde{k} \gamma_\rho}{2p_3 \cdot k} \right),$$

is the matrix element of the virtual electron Compton amplitude.

Similarly the F^{VPC} may be written

$$(II. 7) \quad F^{VPC} = c_2 \bar{u}(p_4) \epsilon''^\mu M_{\mu\nu} \epsilon^\nu u(p_2)$$

where now the index ν refers to the real photon,

$$(II. 8) \quad \mathcal{E}_{\mu}'' = \frac{1}{v^2} \bar{u}(p_2) \gamma_{\mu} u(p_1)$$

and $M_{\mu\nu}$ denote the virtual proton Compton amplitude. Now pure QED can not describe entirely the amplitude $M_{\mu\nu}$. However requiring Lorentz, parity and charge conjugation invariance $M_{\mu\nu}$ can be written⁽⁵⁾ in terms of twelve manifestly gauge invariant amplitudes f_i ($i = 1, \dots, 12$). By keeping the same notation as in ref. (5), one has in our conventions:

$$(II. 9) \quad M_{\mu\nu} = \frac{C_{\mu} C_{\nu}}{MC^2} \left[f_1 + \frac{1}{M} \tilde{K} f_2 \right] + \frac{D_{\mu} D_{\nu}}{MD^2} \left[f_3 + \frac{1}{M} \tilde{K} f_4 \right] + \\ + \frac{M(C_{\mu} D_{\nu} + D_{\mu} C_{\nu})}{D^2} \left[i\gamma_5 f_5 + \frac{1}{M^3} \tilde{D} f_6 \right] + \frac{M(C_{\mu} D_{\nu} - C_{\mu} D_{\nu})}{D^2} \left[i\gamma_5 f_7 + \right. \\ \left. + \frac{1}{M^3} \tilde{D} f_8 \right] + \frac{MA'_{\mu} C_{\nu}}{A^2 C^2} \left[f_9 + \frac{1}{M} \tilde{K} f_{10} \right] + \frac{M^3 A'_{\mu} D_{\nu}}{A^2 D^2} \left[i\gamma_5 f_{11} + \frac{1}{M^3} \tilde{D} f_{12} \right],$$

where A_{μ} , B_{μ} , C_{μ} and D_{μ} are four orthogonal four-vectors, chosen as basic vectors, defined as follows:

$$A_{\mu} = K_{\mu} = \frac{1}{2} (r+k)_{\mu}; \quad Q_{\mu} = \frac{1}{2} (r-k)_{\mu}; \quad R_{\mu} = \frac{1}{2} (p_2 + p_4)_{\mu};$$

$$B_{\mu} = Q_{\mu} - \frac{Q \cdot K}{K^2} K_{\mu}; \quad C_{\mu} = R_{\mu} - \frac{R \cdot K}{K^2} K_{\mu} - \frac{R \cdot B}{B^2} B_{\mu};$$

$$D_{\mu} = \epsilon_{\mu\alpha\beta\gamma} A^{\alpha} B^{\beta} C^{\gamma};$$

and $A'_{\mu} = A_{\mu} + x B_{\mu}$ with x defined in the Appendix. As has been shown in ref. (5) the twelve amplitudes f_i are functions of three invariations choosen to be the \mathcal{V}_1 , \mathcal{V}_2 and \mathcal{V}_3 defined in the appendix. In the case that both photons are real the twelve f_i are reduced to the following six f_j ($j=1, 2, 3, 4, 6, 7$).

III. - WIDE ANGLE BREMSSTRAHLUNG CROSS SECTIONS -

The differential cross section for the process (I. 1), in terms of the matrix element F defined in (II. 1) is given by:

6.

$$(III. 1) \quad d\sigma = \frac{1}{(2\pi)^5} \frac{m^2 M^2}{2\sqrt{(p_1 \cdot p_2)^2 - m^2 M^2}} |F|^2 \delta^4(p_1 + p_2 - p_3 - p_4 - k) \frac{d^3 p_3}{E_3} \times \\ \times \frac{d^3 p_4}{E_4} \frac{d^3 k}{k_o},$$

where, due to eq. (II. 2)

$$(III. 2) \quad |F|^2 = |F^{BH}|^2 + |F^{VPC}|^2 + 2\text{Re}(F^{BH})^* \cdot F^{VPC}.$$

We give the explicit expression of (III. 1) in the following particular cases.

A. - Differential cross section, unpolarized target. -

If the polarizations are not observed, we must average over initial, and sum over final, spins.

Then eq. (III. 1) becomes:

$$(III. 3) \quad d\sigma = \frac{M^2 \alpha^3}{2\pi \sqrt{(p_1 \cdot p_2)^2 - m^2 M^2}} \left\{ I_1 + I_2 + I_3 \right\} \delta^4(p_1 + p_2 - p_3 - p_4 - k) \times \\ \times \frac{d^3 p_3}{E_3} \frac{d^3 p_4}{E_4} \frac{d^3 k}{k_o},$$

where $\alpha = \frac{e^2}{4\pi}$, and I_1 , I_2 and I_3 are given by:

$$(III. 4) \quad I_1 = \frac{1}{q^4} \left\{ J_1(q^2) \left[-\frac{\lambda_1}{\lambda_2} \frac{\lambda_2}{\lambda_1} \frac{m^2 q^2}{2\lambda_1^2} - \frac{m^2 q^2}{2\lambda_2^2} - \frac{r^2 q^2}{2\lambda_1 \lambda_2} \right] + J_2(q^2) \left[-\frac{m^2}{2M^2} \left(\frac{\mu_1 + \mu_4}{\lambda_2} - \frac{\mu_2 + \mu_3}{\lambda_1} \right)^2 - \frac{q^2}{4M^2} \left(\frac{(\mu_1 + \mu_4)^2 + (\mu_2 + \mu_3)^2}{\lambda_1 \lambda_2} \right) + \frac{m^2 q^2}{\lambda_1 \lambda_2} \left(1 - \frac{q^2}{4M^2} \right) \right] + J_3(q^2) \left[\left(\frac{m^2}{\lambda_1} - \frac{m^2}{\lambda_2} \right) \frac{1}{2} \left(\frac{m^2}{\lambda_1} - \frac{m^2}{\lambda_2} \right)^2 \right] \right\},$$

with

$$(III. 5) \quad J_1(q^2) = F_1^2 + \frac{1}{4} (F_1^2 + 4F_1 F_2 \mu + F_2^2 \mu^2) \frac{q^2}{M^2} + \frac{\mu^2 F_2^2}{16} \left(\frac{q^2}{M^2} \right)^2,$$

$$(III. 5) \quad \mathcal{F}_2(q^2) \equiv F_1^2 - \frac{\mu^2 q^2}{4M^2} F_2^2, \quad \mathcal{F}_3(q^2) \equiv (F_1 + \mu F_2)^2 \frac{q^2}{M^2};$$

$$(III. 6) \quad I_2 = -\frac{4}{q^2 r^2} \frac{1}{4\sqrt{\frac{v_4^2 - v_2^2}{2}}} \left[(f_1 f_2) y_1 + (f_3, f_4) y_2 + (f_9, f_{10}) y_3 + (F_1 + \mu F_2) \frac{q^2}{M^2} \sum_{n=1}^6 Z_n \operatorname{Re}(f_{2n}) \right],$$

with

$$(III. 7) \quad (f_i, f_j) \equiv F_1(q^2) \operatorname{Re}(f_i + v_1 f_j) + \frac{\mu q^2}{4M^2} F_2(q^2) \operatorname{Re}(f_i);$$

$$(III. 8) \quad I_3 = -\frac{2}{4} \left[\frac{4v_3^2 \alpha_3}{\sqrt{\frac{v_4^2 - v_2^2}{2}}} (4v_4^2 - v_2^2) J_1 + (v_3 + \alpha_1^2 \alpha_3) J_2 + (v_3 + \alpha_2^2) J_3 - (8v_3 v_4 \alpha_1 \alpha_3 / v_2^2) J_4 \right].$$

with

$$(III. 9) \quad J_1 \equiv [9, 10, 11, 12] \equiv |f_9 + v_1 f_{10}|^2 + (v_2 + v_3) \left\{ |f_{12}|^2 - |f_9|^2 - v_2^{-2} |f_{11}|^2 \right\} + \frac{v_1^2 (v_2 + v_3)^2}{v_2^2} |f_{12}|^2 - v_2^2 \left\{ |f_{10}|^2 + \left(\frac{v_2 + v_3}{v_2} \right)^2 |f_{12}|^2 \right\},$$

$$J_2 = [1, 2, 5+7, 6+8], \quad J_3 = [3, 4, 5-7, 6-8],$$

$$J_4 = \operatorname{Re} \left\{ (f_1 + v_1 f_2)(f_9^* + v_1 f_{10}^*) + (v_2 + v_3) \left[f_{12}^* (f_6 + f_8) - f_1 f_9^* - v_2^{-2} f_{11}^* \times (f_5 + f_7) \right] + \frac{v_1^2 (v_2 + v_3)^2}{v_2^2} (f_6 + f_8) f_{12}^* - v_2^2 \left[f_2 f_{10}^* + \left(\frac{v_2 + v_3}{v_2} \right)^2 x \times (f_6 + f_8) f_{12}^* \right] \right\}.$$

In other words I_1 is the BH term, I_2 the interference between BH

8.

and VPC amplitudes and I_3 is the VPC term. The notation used is given in the appendix and it is the same as that of Berg and Lindner⁽⁵⁾ to make easier the comparison of the formulas. The above results are in agreement with those obtained previously by these authors.

In coincidence experiments, in which the quantity

$$\frac{d^5\sigma}{d\Omega_3 d\Omega_4 dE_4} \Big|_{Lab}$$

is measured, the equation (III. 3) becomes:

$$(III. 10) \quad \frac{d^5\sigma}{d\Omega_3 d\Omega_4 dE_4} \Big|_{Lab} = \frac{\alpha^3}{2\pi^2} \frac{M}{k_o} \frac{\vec{p}_3^2}{E_3} \frac{|\vec{p}_4|}{|\vec{p}_1|} \frac{1}{|\vec{p}_3|} \frac{1}{E_3} \frac{\{I_1 + I_2 + I_3\}}{-\hat{p}_3 \cdot \hat{k}}$$

In the case that only one final particle is observed this formula has to be integrated properly.

B. - Differential cross section, polarized target. -

We describe the two possible spin states, of a fermion of momentum p by the covariant projection operators⁽⁷⁾:

$$(III. 11) \quad P(\underline{s}) = \frac{1}{2} (1 \pm \gamma_5 \tilde{s}),$$

where s is the spin of the proton

$$s \cdot p = 0, \quad s^2 = -1 .$$

We consider WAB process in which the initial proton (target) is polarized along s , and we define the quantity

$$(III. 12) \quad R = \frac{d\sigma(+s) - d\sigma(-s)}{d\sigma(+s) + d\sigma(-s)} ,$$

where $d\sigma(\underline{s})$ is the differential cross section of WAB with the two possible spin states. With this definition we find that R is written:

$$(III. 13) \quad R = \frac{\frac{M^2 \alpha^3}{2\pi^2 \sqrt{(p_1 p_2)^2 - m^2 M^2}} \{II_2 + II_3\} \delta^4(p_1 + p_2 - p_3 - p_4 - k) \frac{d^3 p_3}{E_3} \frac{d^3 p_4}{E_4} \frac{d^3 k}{k_o}}{d\sigma_{unpolarized}}$$

where II_2 and II_3 are given by:

$$\Pi_2 = \frac{2}{r^4} \operatorname{Im} \sum_{k=1}^6 \gamma_k N_k,$$

with:

$$\begin{aligned} N_1 &= \frac{\xi \alpha_3}{\sqrt{2}} \left[\frac{4 \nu_3 \nu_4}{\sqrt{2}} (11, 3, 5-7, 9) + \alpha_1 (1, 5-7, 3, 5+7) \right], \\ N_2 &= \frac{\xi \alpha_3}{\sqrt{2}} \left[\frac{4 \nu_3 \nu_4}{\sqrt{2}} (4, 12, 10, 6-8) + \alpha_1 (6-8, 2, 6+8, 4) \right], \\ N_3 &= \frac{\xi \alpha_3}{\sqrt{2}} \left[\frac{4 \nu_3 \nu_4}{\sqrt{2}} (3, 12, 9, 6-8) + \alpha_1 (6-8, 1, 6+8, 3) \right], \\ N_4 &= \frac{\xi \alpha_3}{\sqrt{2}} \left[\frac{4 \nu_3 \nu_4}{\sqrt{2}} (4, 11, 10, 5-7) + \alpha_1 (5-7, 2, 5+7, 4) \right], \end{aligned}$$

(III. 14)

$$\begin{aligned} N_5 &= f_1 f_2^* (\alpha_1^2 \alpha_3 + \nu_3) + f_3 f_4^* (\alpha_2 + \nu_3) - \frac{4 \nu_3 \alpha_3}{\sqrt{2}} \left[\alpha_1 \nu_4 (2, 9, 10, 1) + \right. \\ &\quad \left. + \nu_3 (1 - \frac{4 \nu_4^2}{\sqrt{2}}) f_9 f_{10}^* \right] \equiv \{1, 2, 3, 4, 9, 10\}, \end{aligned}$$

$$N_6 = \frac{1}{\sqrt{2}} \left\{ 6+8, 5+7, 6-8, 5-7, 12, 11 \right\},$$

$$(h, k, l, m) \equiv f_h^* f_k + f_l^* f_m;$$

$$\begin{aligned} \Pi_3 &= \frac{1}{r^2} \frac{1}{q^2} \frac{2}{(4 \nu_4^2 - \nu_2^2)} \left\{ f_1 \phi \left[\sigma_1 \gamma_3 + \left[\sigma_2 \sigma_3 - 4 \alpha_1^2 \alpha_3 \frac{\nu_4}{\sqrt{2}} (\nu_2 + \nu_3) \right] \gamma_5 \right] + \right. \\ &\quad \left. + f_2 \left[\phi \left[\sigma_1 \gamma_2 - \sigma_2 \gamma_5 \right] + F_2 (q^2) \mu \gamma_5 y_1 \right] \right\} + \\ (III. 15) \quad &+ f_3 \phi \left[\sigma_4 \gamma_3 + \left[\sigma_3 \sigma_5 - 4 \alpha_2 \frac{\nu_4}{\sqrt{2}} (\nu_2 + \nu_3) \gamma_5 \right] \right] + \\ &+ f_4 \left[\phi \left[\sigma_4 \gamma_2 - \sigma_5 \gamma_5 \right] + F_2 (q^2) \mu \gamma_5 y_2 \right] + \end{aligned}$$

10.

$$\begin{aligned}
 & +f_5 \left[\emptyset \alpha_3 \left[-\alpha_1 \gamma_6 (\sigma_7 + \frac{4\alpha_2}{\nu_2}) + \gamma_1 \sigma_8 - \gamma_4 \sigma_{14} \right] - F_2(q^2) \mu \sigma_6 \gamma_1 \right] + \\
 & +f_6 \left[F_2(q^2) \mu \sigma_6 \gamma_3 - \emptyset \alpha_3 \left[\gamma_3 \sigma_8 + \gamma_2 \sigma_{14} \right] \right] + \\
 & +f_7 \sigma_{11} \left[-\xi F_2(q^2) \mu \gamma_1 + \emptyset \alpha_3 \left[\alpha_1 \gamma_6 + \xi (\gamma_1 - \sigma_3 \gamma_4) \right] \right] + \\
 & +f_8 \sigma_{11} \left[\xi F_2(q^2) \mu \gamma_3 - \emptyset \alpha_3 \xi \left[\gamma_3 + \sigma_3 \gamma_2 \right] \right] + \\
 (III. 15) \quad & +f_9 \emptyset \left[\left[\dot{\sigma}_3 \sigma_9 - \frac{4(\nu_2 + \nu_3)}{\nu_2^2} Z_5 \right] \gamma_5 - \sigma_{13} \gamma_3 \right] + \\
 & +f_{10} \left[F_2(q^2) \mu y_3 \gamma_5 - \emptyset \left[\sigma_9 \gamma_5 + \sigma_{13} \gamma_2 \right] \right] + \\
 & +f_{11} \left[F_2(q^2) \mu \sigma_{10} \gamma_1 + \emptyset \left[\gamma_4 \sigma_{12} - \frac{4\alpha_3}{\nu_2^2} Z_6 \gamma_6 - \sigma_{13} \gamma_1 \right] \right] + \\
 & +f_{12} \left[-F_2(q^2) \mu \sigma_{10} \gamma_3 + \emptyset \left[\gamma_2 \sigma_{12} + \sigma_{13} \gamma_3 \right] \right]
 \end{aligned}$$

with:

$$\begin{aligned}
 \gamma_1 &= \frac{s \cdot p_4}{M}, \\
 \gamma_2 &= \frac{\nu_2^2}{M} \left\{ \left[1 - \frac{\nu_1}{\nu_2} - \frac{2\nu_1\nu_3}{\nu_2^2} \right] (s \cdot p_4) + \frac{2\nu_1}{\nu_2^2} (\nu_2 + \nu_3) s \cdot r \right\}, \\
 \gamma_3 &= -\frac{1}{M} \left\{ 2s \cdot r (\nu_2 + \nu_3)(\nu_2 + \nu_3 - 1) + s \cdot p_4 \left[\nu_1 (\nu_2 + \nu_3) + (1 - \nu_2 - \nu_3)(2\nu_3 + \nu_2) \right] \right\}, \\
 \gamma_4 &= -\frac{1}{M} \left\{ -2(\nu_2 + \nu_3)s \cdot r + (2\nu_3 + \nu_2 - \nu_1)s \cdot p_4 \right\}, \\
 (III. 16) \quad \gamma_5 &= \frac{2s \cdot D}{M^3}, \\
 \gamma_6 &= -\frac{2}{M^3} (\nu_2 + \nu_3)s \cdot D;
 \end{aligned}$$

$$\phi \equiv F_1(q^2) + \mu F_2(q^2) ;$$

$$\xi \text{ and } \sigma_i (i = 1 \dots 14)$$

are defined in the appendix. Π_2 and Π_3 result respectively from the VPC amplitude and its interference with the BH one. In the numerator of (III. 13) the pure BH term vanishes identically.

From the knowledge of R the ratio

$$(III. 17) \quad \frac{d\sigma(+s)}{d\sigma(-s)} = \frac{1+R}{1-R} ,$$

can be found, which is a more convenient quantity to be measured.

In the laboratory frame and in coincidence measurements R is given by:

$$(III. 18) \quad R = \frac{\frac{e^3}{2\pi^2} \frac{\vec{p}_3^2}{E_3} \frac{M}{k_0} \frac{|\vec{p}_4|}{|\vec{p}_1|} \frac{1}{(|\vec{p}_3|/E_3) - \hat{p}_3 \cdot \hat{k}} \left\{ \Pi_2 + \Pi_3 \right\}}{\frac{d^5\sigma_{\text{unpol.}}}{d\Omega_3 d\Omega_4 dE_4}} \Bigg|_{\text{Lab.}}$$

where:

$$\frac{d^5\sigma_{\text{unpol.}}}{d\Omega_3 d\Omega_4 dE_4} ,$$

has been defined in (III. 10).

C - Polarization of the recoil proton. -

In the previous paragraph we wrote down the expression of R, (eq. III. 11), when the initial proton (target) is polarized and the polarizations of the final particles are not observed. We consider now the case of unpolarized targets and the recoil proton polarization observed.

Likewise we define the quantity

$$(III. 19) \quad R' = \frac{d\sigma(+s) - d\sigma(-s)}{d\sigma(+s) + d\sigma(-s)} ,$$

where now the spin s is referred to the final proton.

R' is obtained from R by redefining the quantities γ_i ($i = 1, \dots, 6$), appearing in (III. 14) and (III. 15) as follows:

$$\begin{aligned}
 \gamma_1 &= -\frac{\mathbf{s} \cdot \mathbf{p}_2}{M}, \\
 \gamma_2 &= \frac{\nu_2^2}{M} \left\{ \left[1 + \frac{\nu_1}{\nu_2} + \frac{2\nu_1\nu_3}{\nu_2^2} \right] \mathbf{s} \cdot \mathbf{p}_2 + \frac{2\nu_1}{\nu_2^2} (\nu_2 + \nu_3) \mathbf{s} \cdot \mathbf{r} \right\}, \\
 \gamma_3 &= -\frac{1}{M} \left\{ 2\mathbf{s} \cdot \mathbf{r} (\nu_2 + \nu_3)(\nu_2 + \nu_3 - 1) - \mathbf{s} \cdot \mathbf{p}_2 \left[(1 - \nu_2 - \nu_3)(2\nu_3 + \nu_2) - \right. \right. \\
 &\quad \left. \left. - \nu_1(\nu_2 + \nu_3) \right] \right\}, \\
 \gamma_4 &= \frac{2}{M} (\nu_2 + \nu_3) \mathbf{s} \cdot \mathbf{r} + \frac{1}{M} (2\nu_3 + \nu_2 + \nu_1) \mathbf{s} \cdot \mathbf{p}_2, \\
 \gamma_5 &= \frac{2}{M^3} \mathbf{s} \cdot \mathbf{D}, \\
 \gamma_6 &= \frac{2}{M^3} (\nu_2 + \nu_3) \mathbf{s} \cdot \mathbf{D},
 \end{aligned} \tag{III. 20}$$

and all the rest unchanged.

IV. - VIRTUAL PROTON COMPTON CONTRIBUTION TO THE WAB. -

In Section II the VPC amplitude $M_{\mu\nu}$ has been written in terms of the twelve amplitudes f_i ($i = 1, \dots, 12$). We now proceed to find their explicit expressions. To achieve this we approximate the blob of Fig. 1 (c) by the contributions of a single virtual proton and a 3-3 resonance. This approximation limits our predictions to the experimental configuration in which only these states are relevant. We dismiss also π^0 and η^0 exchange contributions since it is known that they are almost negligible at and below the first resonance^(5, 8).

A. - Single nucleon intermediate state. -

The contribution of the single nucleon intermediate state to the f_i 's may be found by using unitarity in the manner described by Hearn and Leader but this procedure does not guarantee the correct low energy limit⁽⁹⁾.

Instead we appeal to the low-energy Compton scattering theorem⁽¹⁰⁾ which states that the low-energy limit is correctly given by the lowest order perturbation theory, if anomalous Pauli moments are included. Accordingly the single nucleon contribution is given by:

$$(IV. 1) \quad M_{\mu\nu}^B = (\gamma_\nu + \frac{\mu}{2M} \gamma_\nu \tilde{k}) \frac{\tilde{p}_2 + \tilde{r} + M}{(\tilde{p}_2 + \tilde{r})^2 - M^2} \left[F_1(r^2) \gamma_\mu + \frac{\mu}{4M} F_2(r^2) (\tilde{r} \gamma_\mu - \gamma_\mu \tilde{r}) \right] +$$

+ crossed term.

Now taking into account that A, B, C and D form an orthogonal basis and that $M_{\mu\nu} \sim$ operates between two free proton Dirac spinors, and using the identity $D = i\gamma_5 \tilde{A} \tilde{B} \tilde{C}$, we find that:

$$(IV. 2) \quad f_1^B = \frac{2 \sqrt{2} F_1(r^2)}{\sqrt{v_1^2 - v_2^2}} - \frac{2 \sqrt{3} \mu F_2(r^2)}{\sqrt{v_2^2}},$$

$$f_2^B = \frac{\sqrt{v_1} F_1(r^2)}{\sqrt{v_1^2 - v_2^2}} + \frac{2 \sqrt{v_1} \sqrt{3} (F_1(r^2) + \mu F_2(r^2))}{\sqrt{v_2} (\sqrt{v_1^2 - v_2^2})},$$

$$f_3^B = \mu \left[F_1(r^2) + (1+\mu) F_2(r^2) \right],$$

$$f_4^B = - \frac{\sqrt{v_1}}{\sqrt{v_1^2 - v_2^2}} (1+\mu) \left[F_1(r^2) \mu F_2(r^2) \right],$$

$$f_5^B = - \frac{\mu}{2} \left[F_2(r^2) - F_1(r^2) \right] \sqrt{v_2} \cdot \frac{(\sqrt{v_1^2 - v_2^2})(\sqrt{v_2 + v_3}) + v_2^2}{(\sqrt{v_2 + v_3})(\sqrt{v_1^2 - v_2^2})},$$

$$f_6^B = \sqrt{v_2} \frac{2 F_1(r^2) + \mu [F_1(r^2) + F_2(r^2)]}{2(v_1^2 - v_2^2)} + \frac{\sqrt{v_2} \sqrt{3} \mu [F_2(r^2) - F_1(r^2)]}{2(v_1^2 - v_2^2)(\sqrt{v_2 + v_3})} -$$

$$- \frac{1}{2} \mu^2 F_2(r^2),$$

$$f_7^B = \frac{\sqrt{v_2}^3 [2 F_1(r^2) + \mu (F_1(r^2) + F_2(r^2))]}{2(\sqrt{v_2 + v_3})(\sqrt{v_1^2 - v_2^2})} - \mu^2 F_2(r^2) \frac{\sqrt{v_2} \sqrt{3}}{2(\sqrt{v_2 + v_3})} - \frac{\mu}{2} \sqrt{v_2} \cdot$$

$$\cdot \left[F_1(r^2) + F_2(r^2) + \mu F_2(r^2) \right],$$

$$f_8^B = -\frac{\mu^2}{2} F_2(r^2) \frac{\sqrt{3}}{\sqrt{2} + \sqrt{3}} + \frac{\sqrt{2}^2}{2(\sqrt{1}^2 - \sqrt{2}^2)(\sqrt{2} + \sqrt{3})} \times$$

$$\times \left[2F_1(r^2) + \mu(F_1(r^2) + F_2(r^2)) \right] - \frac{\sqrt{2} \left[F_1(r^2) + \mu F_2(r^2) \right]}{\sqrt{1}^2 - \sqrt{2}^2},$$

$$f_9^B = -\mu F_2(r^2) \sqrt{1} \left(\frac{1}{2} + \frac{\sqrt{2}}{\sqrt{1}^2 - \sqrt{2}^2} + \frac{\sqrt{3}}{\sqrt{2}^2} \right),$$

$$(IV. 2)$$

$$f_{10}^B = (F_1(r^2) + \mu F_2(r^2)) \left[\frac{\sqrt{2} + \sqrt{3}}{\sqrt{2}} + \frac{\sqrt{2}}{\sqrt{1}^2 - \sqrt{2}^2} \right] - \frac{\sqrt{1}^2 \mu F_2(r^2)}{2(\sqrt{1}^2 - \sqrt{2}^2)},$$

$$f_{11}^B = -\mu(1+\mu)F_2(r^2) \frac{\sqrt{1}\sqrt{2}}{2} \left[1 + \frac{\sqrt{2}^2}{(\sqrt{2} + \sqrt{3})(\sqrt{1}^2 - \sqrt{2}^2)} \right],$$

$$f_{12}^B = -\mu(1+\mu)F_2(r^2) \frac{\sqrt{1}\sqrt{2}^2}{2(\sqrt{2} + \sqrt{3})(\sqrt{1}^2 - \sqrt{2}^2)} - \mu^2 F_2(r^2) \frac{\sqrt{1}}{2}.$$

Apart from f_8^B , these results agrees with those of ref. (5).

B. - Meson-nucleon intermediate state. -

We now have to find the contributions of the meson-nucleon intermediate states. To face this problem the usual analysis using dispersion techniques is not suitable because it leads to excessively complicated calculations. Instead we use an isobaric model for the 3-3 resonance. This resonance can be excited electromagnetically by the magnetic dipole M1, transverse electric quadrupole E2 and scalar quadrupole Q2 transitions. The first alone is well known to give a fairly adequate fit to scattering data and so we have neglected the E2 and Q2 excitations. The magnetic dipole isobaric formation can be described by making use of the well known spin 3/2 partial wave amplitude in the so called nonrelativistic form, and by transforming it into a covariant analytic amplitude, as has been done in ref. (11). However, since up to now we have used the familiar Dirac 4-spinor formalism, in order to maintain uniformity of our work, we shall employ the Rarite-Schwinger spin 3/2 propagator and vertex function. As interaction for the $\gamma p N^*$ vertex we choose⁽¹²⁾:

$$(IV. 3) \quad H = \frac{eg}{\Delta} \bar{\Psi}_5(x) \gamma_5 \gamma_\mu \phi(x) F_{\mu\nu} + h.c.,$$

where $\phi(x)$ is the proton field, $F_{\mu\nu}$ is the electromagnetic field tensor and $\bar{\Psi}_5(x)$ is the spin 3/2 field of Rarita and Schwinger; and as spin 3/2 propagator:

$$(IV. 4) \quad S_{\mu\nu}(p) = \frac{\tilde{p} + \Delta}{p^2 - \Delta^2 + i\Gamma} \left\{ g_{\mu\nu} - \frac{\gamma_\mu \gamma_\nu}{3} - \frac{1}{3\Delta} (\gamma_\mu p_\nu - p_\mu \gamma_\nu) - \frac{2}{3\Delta^2} p_\mu p_\nu \right\},$$

where Δ and p are the mass and the four-momentum of the isobar respectively and g is a dimensionless quantity, the numerical value of which must be obtained from experiment. Γ provides the finite width of the 3-3 resonance; it is chosen such that the half-width at half-maximum $\Gamma/\Delta = (0.125 \pm 0.015)$ GeV. In the case that the photon is off the mass shell g is replaced by $gG(r^2)$ with $G(0) = 1$, where $G(r^2)$ plays the role of the form factor for the γNN^* vertex. The choice of this propagator avoids the presence of an undesirable pole in the crossed diagram but it has the limitation that outside the resonance region it no longer represents a pure angular momentum 3/2 propagator.

In analogy with the equation (IV. 1) we have now for the amplitude $M_{\mu\nu}^{33}$:

$$(IV. 5) \quad M_{\mu\nu}^{33} = \left(\frac{g}{\Delta} \right)^2 G(r^2) \left\{ (g_{\nu\rho} k_\lambda - k_\rho g_{\nu\lambda}) \gamma_5 \gamma_\lambda S_{\rho\sigma}(p_4 + k) \gamma_5 \gamma_\sigma (g_{\mu\sigma} r_\nu - g_{\mu\eta} r_\sigma) \right\} + \\ + \text{crossed term.}$$

By using the same technique as in the single nucleon case we obtain:

$$f_1^{33} = T(s) \left\{ \frac{M^2}{\Delta^2} (\nu_1 - \nu_2) \left[\frac{4}{3} \left(1 - \frac{\nu_1 \nu_3}{\nu_2} \right) + (\nu_1 - \nu_2) \left(2 - \frac{4}{3} \frac{\Delta}{M} \right) \right] + \right. \\ \left. + \left[\frac{2}{3} \frac{\Delta}{M} (\nu_1 + 2\nu_2) - 2\nu_1 \right] \right\},$$

$$(IV. 6) \quad f_2^{33} = T(s) \left\{ \frac{4}{3} \frac{M^2}{\Delta^2} \left[(\nu_2 - \nu_1 - 1) \left[1 + \frac{(\nu_1 - \nu_2)(\nu_2 + \nu_3)}{\nu_2} \right] + \right. \right. \\ \left. \left. + \frac{1}{2} (\nu_1 - \nu_2)(2\nu_3 + \nu_1 - \nu_2) + \frac{\nu_1 \nu_3}{\nu_2} + \frac{\Delta}{M} (\nu_3 + \nu_1 - \nu_2) \right] \right\} +$$

16.

$$+ \frac{2}{3} \left[3 + 2 \nu_3 - \frac{(\nu_2 + 2 \nu_3)(\nu_1 + 2 \nu_2)}{\nu_2} - \frac{\Delta}{M} \right] \},$$

$$\begin{aligned} f_3^{33} = & \frac{2}{3} T(s) \left\{ \frac{M^2}{\Delta^2} (\nu_1 - \nu_2) \left[(2\nu_3 + \nu_1 - \nu_2) + \frac{2\Delta}{M} (\nu_2 - \nu_1) \right. \right. \\ & \left. \left. + (1 + \frac{\Delta}{M})(\nu_1 + 2 \nu_2) \right] \right\}, \end{aligned}$$

$$\begin{aligned} f_4^{33} = & \frac{2}{3} T(s) \left\{ \frac{M^2}{\Delta^2} (\nu_1 - \nu_2) \left[2\frac{\Delta}{M} + (2\nu_3 + \nu_1 - \nu_2) + 2\frac{\Delta}{M} \frac{\nu_3}{\nu_1 - \nu_2} \right] \right. \\ & \left. + (2\nu_3 + \nu_1 + 2\nu_2) - (1 + \frac{\Delta}{M}) \right\}, \end{aligned}$$

$$f_5^{33} = \frac{4}{3} T(s) \frac{M^2}{\Delta^2} \nu_3 \left[\frac{\nu_2^2}{\nu_2 + \nu_3} + (\nu_1^2 - \nu_2^2) \right],$$

$$f_6^{33} = \frac{4}{3} T(s) \left\{ \frac{M^2}{\Delta^2} \left[(\nu_1 - \nu_2)(1 + \nu_1 - \nu_2) + \frac{\nu_2 \nu_3}{\nu_2 + \nu_3} \right] - (\nu_2 + 2\nu_1) \right\},$$

(IV. 6)

$$\begin{aligned} f_7^{33} = & -\frac{4}{3} T(s) \left\{ \frac{\nu_2^2}{\nu_2 + \nu_3} \left[\frac{M^2}{\Delta^2} \left[\nu_3(1 + \frac{2\Delta}{M}) + (\nu_1 - \nu_2)(1 + 2\nu_3 + \nu_1 - \nu_2) \right] \right. \right. \\ & \left. \left. + (2\nu_3 + 5\nu_2 - 2\nu_1) \right] + \frac{M^2}{\Delta^2} (\nu_1 - \nu_2)^2 \left[\nu_2(1 - \frac{2\Delta}{M}) - \nu_3 \right] + \nu_2(1 + \frac{\Delta}{M}) \cdot \right. \\ & \left. \cdot (\nu_1 - 4\nu_2) \right\}, \end{aligned}$$

$$f_8^{33} = \frac{4}{3} T(s) \frac{\nu_3}{\nu_2 + \nu_3} \left\{ \frac{M^2}{\Delta^2} \left[(\nu_1 - \nu_2)(1 + \nu_1 - 3\nu_2) - \nu_2(1 + \frac{2\Delta}{M}) \right] + (3\nu_2 - 2\nu_1) \right\},$$

$$\begin{aligned} f_9^{33} = & \frac{2}{3} T(s) (\nu_1 - \nu_2) \left\{ \frac{M^2}{\Delta^2} (\nu_1 - \nu_2) \left[1 + \nu_1(1 - \frac{\nu_3}{\nu_2}) - (\nu_2 + \nu_3) - \frac{\Delta}{M} \right] \right. \\ & \left. \cdot (\nu_1 + 2\nu_2) \right] - (\nu_2 + 2\nu_1) + (1 + \frac{\Delta}{M}) \frac{\nu_1 + \nu_2}{2} \right\}, \end{aligned}$$

$$f_{10}^{33} = \frac{2}{3} T(s) \left\{ \frac{M^2}{\Delta^2} \left[(\nu_1 - \nu_2) \left[(\nu_3 - 1) - 2(\nu_1 - \nu_2) - (1 + \frac{\nu_3}{\nu_2}) (\nu_1 - \nu_2)^2 \right] + \right. \right.$$

$$\left. \left. \frac{\Delta}{M} \left[\nu_2 + (\nu_1 - \nu_2)(\nu_1 + \nu_2 + \nu_3) \right] \right] + (\nu_1 - \nu_2) \times \right.$$

$$\left. \times \left[2 - \nu_1 - 2\nu_2 - \nu_3 \left(\frac{\nu_1}{\nu_2} - 2 \right) \right] - \frac{1}{2} \nu_1 (1 + \frac{\Delta}{M}) \right\},$$

(IV. 6)

$$f_{11}^{33} = -T(s) \left(\frac{\nu_2^2}{\nu_2 + \nu_3} + \nu_1^2 - \nu_2^2 \right) \left\{ \frac{2}{3} \frac{M^2}{\Delta^2} (\nu_1 - \nu_2) \left(-\frac{\Delta}{M} \nu_2 - \nu_3 \right) + \frac{1}{3} \nu_2 (1 + \frac{\Delta}{M}) \right\},$$

$$f_{12}^{33} = \frac{2}{3} T(s) \left\{ \frac{M^2}{\Delta^2} (\nu_1 - \nu_2) \left[\nu_1 + (\nu_1 - \nu_2)^2 - \frac{\nu_2}{\nu_2 + \nu_3} (\nu_2 + \frac{\Delta}{M} \nu_3) \right] - \right. \\ \left. - (1 + \frac{\Delta}{M}) \frac{\nu_2^2}{2(\nu_2 + \nu_3)} - (\nu_1 - \nu_2)(2\nu_1 + \nu_2) \right\},$$

where:

$$(IV. 7) \quad T(s) = G(r^2) \left(\frac{g}{\Delta} \right)^2 \frac{M^4}{s - \Delta^2 + i\Gamma}$$

and ^(x) $s = M^2(1 + 2(\nu_1 - \nu_2))$. The crossed terms are obtained as follows:

$$f_i(\nu_1, \nu_2, \nu_3) \xrightarrow{\text{crossed}} -f_i(-\nu_1, \nu_2, \nu_3), \quad (i=2, 4, 9, 11, 12)$$

$$f_i(\nu_1, \nu_2, \nu_3) \xrightarrow{\text{crossed}} f_i(-\nu_1, -\nu_2, \nu_3), \quad (i=1, 3, 5, 6, 7, 8, 10).$$

Correct p-wave threshold behaviour implies also that Γ should be multiplied by a suitable kinematical factor which we choose to be $(q/q_r)^3$, where q is the momentum of the decaying pion $N^* \rightarrow \pi^+ N$ in the rest system of the N^* and q_r is the value of q at the resonance⁽¹³⁾.

In order to specify completely the expression of $T(s)$, the values of g^2 and $G(r^2)$ are needed. To evaluate g^2 we make use of the existing expe

(x) - This s should not be confused with the s of the chapter III referred to the spin.

perimental data on the non polarized differential cross-section for Compton scattering at 90° . From the amplitudes (IV. 6) we take the six which contribute to the real Compton effect f_i ($i = 1, 2, 3, 4, 6, 7$), and we consider the contribution of the 3-3 resonance at $r^2 = 0$.

We thus calculate the $(d\sigma/d\Omega)_{90^\circ}$ of the real Compton scattering at the first resonance ($s = \Delta^2$). If in this expression the experimental value⁽¹⁴⁾

$$\left(\frac{d\sigma}{d\Omega}\right)_{90^\circ} = (1.6 \pm 0.2)10^{-31} \text{ cm}^2,$$

is inserted, we obtain

$$g = 2.15 \pm 0.07 .$$

As can be seen from eq. (IV. 3), the constant g has the same meaning as $C_3(0)$ of ref. (12), but it is differently renormalized. In common normalization (used by previous authors) this value becomes $g = 0.298 \pm 0.009$; which should be compared with the values of

$$C_3(0) = 0.37^{(12)}, \quad C_3(0) = 0.298^{(15)}, \quad g = 0.29^{(11)} \text{ and } C_3(0) = 0.3^{(13, 16)}.$$

This agreement provides a check on our calculations. To complete the determination of the covariant isobaric contribution to the virtual Compton scattering amplitude, we have to known the explicit expression of $G(r^2)$. We have used two expressions for it. The first (choice 1) is that given by Durner and Tsai⁽¹³⁾.

$$(IV. 8) \quad G^2(r^2) = e^{-6.3\sqrt{-r^2}} (1 + 9.0\sqrt{-r^2}) .$$

The second (choice 2) is the empirical nucleon isovector magnetic form factor⁽¹⁸⁾. This seemed reasonable since the resonance is excited by an isovector magnetic dipole transition.

V. - NUMERICAL CALCULATIONS AND RESULTS -

With the formulation described in chapters III and IV we are ready to proceed to the numerical calculations. Since no approximations has been made about the mass of the probe particle, the formalism described in the previous chapters is applicable for electron as well as for muons. As examples we have specifically calculated first the quantity⁽¹⁷⁾

$$(d^5\sigma_{\text{unpol}}/d\Omega_3 d\Omega_4 dE_4)/_{\text{Lab}} ,$$

and second the quantities R and R' for the coincidence experiments in WAB, for two initial electron energies 0.9 and 5 GeV, in various experimental configurations.

The kinematics are fixed by the following five parameters: E_1 , E_4 , k_o and u_1 and u_2 , where $u_1 = -(p_1-k)^2$ and $u_2 = -(p_3+k)^2$ are the square of the masses of the two virtual electron states in the Bethe-Heitler graphs.

In Fig. 2a, 2b and 2c we show $d^5\sigma/d\Omega_3 d\Omega_4 dE_{4\text{Lab}}$ as a function of u_1 for fixed $E_1 = 0.90$ GeV and for various E_4 , k_o and u_2 . In Fig. 3a, 3b and 3c we show the same quantity but with $E_1 = 5.0$ GeV. Fig. 2a and 3a, 2b and 3b, 2c and 3c correspond to the case in which the invariant mass of the intermediate protons is 1.150 GeV, 1.236 GeV and 1.350 GeV respectively. If instead of using electrons as a probe we had used muons the results shown in Fig. 2a, 2b and 2c are changed slightly while those shown in Fig. 3a, 3b and 3c remain practically the same. For comparison see table I. From these figures we can make the following observations :

TABLE I

Comparison between e-p and μp bremsstrahlung cross sections:
I, II and III denote respectively the quantities shown in curves I,
II and III of Fig. 2a.

$E_1 = 0.9 \text{ GeV}, E_4 = 1.05 \text{ GeV}, k_o = 0.413 \text{ GeV}$		$E_1 = 10.0 \text{ GeV}, E_4 = 5.54 \text{ GeV}, k_o = 0.358 \text{ GeV}$	
$u_1 = 0.28 \text{ GeV}^2$	$u_1 = 0.26 \text{ GeV}^2$	$u_1 = 2.35 \text{ GeV}^2$	$u_1 = 2.34 \text{ GeV}^2$
$u_2 = -0.40 \text{ GeV}^2$	$u_2 = -0.41 \text{ GeV}^2$	$u_2 = -2.38 \text{ GeV}^2$	$u_2 = -2.39 \text{ GeV}^2$
$(e^-), \mu b/(sr)^2 \text{ GeV}$	$(\mu^-), \mu b/(sr)^2 \text{ GeV}$	$(e^-), \mu b/(sr)^2 \text{ GeV}$	$(\mu^-), \mu b/(sr)^2 \text{ GeV}$
a 0.10584×10^{-3}	0.10264×10^{-3}	0.15188×10^{-6}	0.15188×10^{-6}
b 0.26262×10^{-3}	0.24978×10^{-3}	0.49779×10^{-3}	0.49848×10^{-3}
c 0.25596×10^{-2}	0.23777×10^{-2}	0.10828	0.10825

a) the contributions of the VPC effect depends strongly on the kinematical configuration of the experiments and may change appreciably the results of pure QED in the critical region where the intermediate electron or muon is far off its mass shell;

b) at small momentum transfers to the proton the results obtained with the two form factors (choice 1) and (choice 2) used above substantially agree, (see Fig. 2) while in the large momentum transfer region they strongly differ (see Fig. 3).

These results suggest that the exponential form factor is a more reasonable one, to describe the behavior of the γNN^* vertex form factor, in agreement with the conclusions of the analysis of the electroproduction of pions(13). A coincidence measurement of the WAB in the kinematical configuration of Fig. 3b, for example, in which the BH contribution is negligible by comparison to the VPC term, may decide for this suggestion.

It should be notice that from our calculations result that the crossed graph is negligibly small at the resonance peak, but its relative magnitude is increasing as one goes outside the resonance, and there are kinematical regions where the two graphs give comparable contributions.

Let us deal now with the polarized cross sections. To define the kinematical configurations for the quantities R and R' , in addition to the five invariants chosen for the unpolarized cross section the orientation of the spin is needed. From now on we denote by s_2 and s_4 the spin four-directions of the target and recoil proton respectively. We have choosen our coordinates as follows:

$$\begin{aligned}
 p_1 &= (E_1, |\vec{p}_1|, 0, 0), & p_2 &= (M, 0, 0, 0), \\
 p_3 &= (E_3, |\vec{p}_3| \cos\theta_e, |\vec{p}_3| \sin\theta_e \cos\varphi, |\vec{p}_3| \sin\theta_e \sin\varphi), \\
 (V.1) \quad p_4 &= (E_4, |\vec{p}_4| \cos\theta_p, |\vec{p}_4| \sin\theta_p, 0), \\
 r &= (E_1 - E_3, |\vec{p}_1| - |\vec{p}_3| \cos\theta_e, -|\vec{p}_3| \sin\theta_e \cos\varphi, -|\vec{p}_3| \sin\theta_e \sin\varphi);
 \end{aligned}$$

and

$$(V.2) \quad s_2^x = (0, 1, 0, 0), \quad s_2^y = (0, 0, 1, 0), \quad s_2^z = (0, 0, 0, 1);$$

$$(V.3) \quad \left\{
 \begin{array}{l}
 s_4^{\parallel} = (|\vec{p}_4|, E_4 \cos\theta_p, E_4 \sin\theta_p, 0)/M, \\
 s_4^{\perp} = (0, \sin\theta_p, -\cos\theta_p, 0), \\
 s_4^z = (0, 0, 0, 1),
 \end{array}
 \right.$$

where the angles θ_e , θ_p and φ are shown in Fig. 4.

The expressions for the products occuring in the (II.16) and (III.21) can now be obtained in terms of the angles θ_e , θ_p and φ and initial and final energies. In the Tables II and III we show the results.

TABLE II

The invariants $s_2 \cdot p_4$, $s_2 \cdot r$ and $s_2 \cdot D$ expressed in terms of momentum and angles for various choices of the polarization s_2 . Quantities evaluated in the laboratory frame (Fig. 4).

$s_2^x \cdot p_4$	$= - \tilde{p}_4 \cos \theta_p$
$s_2^y \cdot p_4$	$= - \tilde{p}_4 \sin \theta_p$
$s_2^z \cdot p_4$	$= 0$
$s_2^x \cdot r$	$= \tilde{p}_3 \cos \theta_e - \tilde{p}_1 $
$s_2^y \cdot r$	$= \tilde{p}_3 \sin \theta_e \cos \psi$
$s_2^z \cdot r$	$= \tilde{p}_3 \sin \theta_e \sin \psi$
$s_2^x \cdot D$	$= -\frac{M}{2} \tilde{p}_3 \tilde{p}_4 \sin \theta_e \sin \theta_p \sin \psi$
$s_2^y \cdot D$	$= \frac{M}{2} \tilde{p}_3 \tilde{p}_4 \cos \theta_p \sin \theta_e \sin \psi$
$s_2^z \cdot D$	$= \frac{M}{2} \left\{ \tilde{p}_3 \tilde{p}_4 (\cos \theta_e \sin \theta_p - \cos \theta_p \sin \theta_e \cos \psi) - \tilde{p}_1 \tilde{p}_4 \sin \theta_p \right\}$

TABLE III

The same as Table II with s_2 replaced by s_4 .

$s_4^0 \cdot p_2$	$= \tilde{p}_4 $
$s_4^1 \cdot p_2$	$= 0$
$s_4^2 \cdot p_2$	$= 0$
$s_4^0 \cdot r$	$= \frac{ \tilde{p}_4 }{M} (E_1 - E_3) + \frac{E_4}{M} (\tilde{p}_3 \cos \theta_e \cos \theta_p + \tilde{p}_3 \sin \theta_e \sin \theta_p \cos \psi - \tilde{p}_1 \cos \theta_p)$
$s_4^1 \cdot r$	$= \frac{1}{M} (\tilde{p}_3 \cos \theta_e \sin \theta_p - \tilde{p}_3 \sin \theta_e \cos \theta_p \cos \psi - \tilde{p}_1 \sin \theta_p)$
$s_4^2 \cdot r$	$= \tilde{p}_3 \sin \theta_e \sin \psi$
$s_4^0 \cdot D$	$= 0$
$s_4^1 \cdot D$	$= -\frac{M}{2} \tilde{p}_3 \tilde{p}_4 \sin \theta_e \sin \psi$
$s_4^2 \cdot D$	$= \frac{M}{2} \left[\tilde{p}_3 \tilde{p}_4 (\cos \theta_e \sin \theta_p - \cos \theta_p \sin \theta_e \cos \psi) - \tilde{p}_1 \tilde{p}_4 \sin \theta_p \right]$

In the above coordinate system $\vec{\xi}$ is given by

$$(V.4) \quad \vec{\xi} = \frac{1}{2M^3} \vec{p}_4 \cdot (\vec{p}_1 \times \vec{p}_3) = - \frac{|\vec{p}_1| |\vec{p}_3| |\vec{p}_4| \sin\theta_e \sin\theta_p \sin\varphi}{2M^3}$$

Let us choose now as orientation of the spin target and of spin of the observed recoil proton the s_2^y and s_4^z respectively. For these particular choices we report in Fig. 5a and 5b R as a function of u_1 and the rest of the kinematics is as in Fig. 2b and 3b respectively.

In Figg. (6a) and (6b), R' is plotted under the same circumstances as the previous Fig. (5a) and (5b) respectively. As we see from these figures, large polarization effects arise. We observe again that in the large momentum transfer region, R and R' are strongly dependent on $G(r^2)$ and a measurement of R and R' can provide information about this form factor as well as about the VPC amplitude.

In experiments in which both e^+ and e^- are available, also the interference between BH and VPC amplitude may be avoided in the numerators of R and R' , provided that respectively the polarization of the target and the polarization of the recoil proton does remain the same.

Thus the WAB experiments with polarized targets or in which the polarization of the recoil protons is measured, provide us a good source of information about VPC amplitude.

This aim can be better achieved⁽¹⁹⁾ in the large-angle pair photo-production experiments, if similar polarization measurements are made. In this case it is easy to see that in a symmetrical arrangement where charges and polarization of the final leptons are not observed, only the VPC amplitude contributes to the numerators of R and R' . A clarification of the importance of the VPC term in this process would be valuable, because in many current theoretical interpretations of these measurements, the contribution of the nucleon isobars has been considered, in poorly justified approximations, negligibly small⁽²⁰⁾.

V. - DISCUSSION -

By using the covariant isobaric formalism we have been able to avoid the difficulties that arise in the present problem if dispersion relations are used. The results are of course model dependent. However, other experiments indicate that the model we have assumed should give the bulk of the VPC effect on the WAB experiments. The approximations that have been made are such that the predictions are limited to the experimental configurations in which only the single nucleon and the 3-3 resonance intermediate states are relevant; that is when the invariant mass

of the intermediate proton is not far above the first resonance. Under that predictions it is legitimate to neglect the contributions of π^0 and γ^0 exchange⁽⁸⁾.

In our analysis we have dismissed the possible contributions from E2 and Q2. The former transitions is well known from the scattering data to give a very small contribution in comparison to M1, while from the data of electroproduction one cannot say exactly how much contributes the latter one. Nevertheless there are well based arguments which suggest that Q2 cannot be large⁽¹³⁾. So it is believed that the inclusion of E2 and Q2 should not change the striking features of our results. These features as we noted above are the strong dependence of the VPC effect a) on the kinematical configuration of the WAB experiment and b) on the form factor $G(r^2)$ appropriate to the vertex γNN^* . From the numerical results we concluded that the $G(r^2)$ given by Dufner and Tsai seems more realistic than the empirical isovector magnetic form factors. It should be noted that this conclusion is not affected from the approximation to ignore E2 and Q2 because if for example the Q2 transition were significant, the form factor $G(r^2)$ must decrease still faster than that of Dufner and Tsai⁽¹³⁾.

The question of the radiative corrections detected experimentally⁽²⁰⁾ in the process (I. 1) has not been faced in this paper and it has to be considered separately.

From the present calculations results that as smaller distances are probed (as the off mass shell of electron (muon) increase) the contributions arising from the VPC effect are relatively increasing.

ACKNOWLEDGMENTS -

We wish to thank Professors Nicola Cabibbo and Bruno Touschek for many stimulating discussions. One of us (A. V.) is grateful to the Istituto di Fisica dell'Università di Roma and to the Laboratori del CNEN di Frascati for their support ~~and~~^{and} kind hospitality. He is also indebted to Professor B. De Tolla for several interesting and helpful discussions.

APPENDIX -

Following ref. (5) we consider the amplitudes f_i to be functions of the three invariants: γ_1 , γ_2 and γ_3 defined as follows:

$$\gamma_1 \equiv \frac{R \cdot K}{M^2}, \quad \gamma_2 \equiv \frac{Q^2 - K^2}{2M^2}, \quad \gamma_3 \equiv \frac{Q \cdot K}{M^2} = \frac{r^2}{4M^2} .$$

We also define

$$\gamma_4 \equiv \frac{(\Lambda \cdot A)}{M^2} = \frac{\lambda_1 + \lambda_2}{4M^2} = \frac{(k \cdot p_1) + (k \cdot p_2)}{4M^2} \quad \text{and}$$

$$\gamma_5 = \frac{(\Lambda \cdot R)}{M^2} = \frac{(p_1 + p_3) \cdot (p_2 + p_4)}{4M^2}, \quad \text{where} \quad \Lambda = \frac{1}{2}(p_1 + p_3).$$

The variables appearing in the formulas of unpolarized and polarized cross sections are expressed in terms of the γ 's as follows:

$$x = (\gamma_3 - \gamma_2)(2\gamma_3 - \gamma_2)/\gamma_2^2,$$

$$\lambda_1 = (k \cdot p_1) = M^2(2\gamma_4 - \gamma_2),$$

$$\lambda_2 = (k \cdot p_2) = M^2(2\gamma_4 + \gamma_2),$$

$$r^2 = (p_1 - p_3)^2 = 4M^2\gamma_3,$$

$$q^2 = (p_2 - p_4)^2 = 4M^2(\gamma_2 + \gamma_3),$$

$$\mu_1 = (p_1 \cdot p_2) = M^2 \left[\gamma_5 + \gamma_4 - \gamma_3 - \frac{1}{2}(\gamma_2 - \gamma_1) \right],$$

$$\mu_2 = (p_3 \cdot p_4) = M^2 \left[\gamma_5 - \gamma_4 - \gamma_3 - \frac{1}{2}(\gamma_2 + \gamma_1) \right],$$

$$\mu_3 = (p_1 \cdot p_4) = M^2 \left[\gamma_5 + \gamma_4 + \gamma_3 + \frac{1}{2}(\gamma_2 - \gamma_1) \right],$$

$$\mu_4 = (p_2 \cdot p_3) = M^2 \left[\gamma_5 - \gamma_4 + \gamma_3 + \frac{1}{2}(\gamma_2 + \gamma_1) \right];$$

$$\alpha_1 = \nu_5 + \nu_1 \nu_4 (2 \nu_3 + \nu_2) / \nu_2^2,$$

$$\alpha_2 = \frac{(\Lambda \cdot D)^2}{M^2 D^2} = \left(\frac{m^2}{M^2} - \nu_3^2 \right) + \frac{M^6}{D^2} \left[- (\nu_2 \nu_5 + \nu_1 \nu_4)^2 + 4 \nu_3 (\nu_4^2 - \nu_1 \nu_4 \nu_5) - 4 \nu_3 \nu_4^2 (\nu_2 + \nu_3) \right],$$

$$\alpha_3 = \nu_2^2 \left[\nu_2^2 + (\nu_2 + \nu_3)(\nu_1^2 - \nu_2^2) \right]^{-1},$$

$$D^2 = M^6 \nu_2^2 / \alpha_3,$$

$$\mathfrak{Z} = \frac{1}{2} \epsilon_{\alpha \beta \rho \mu} p_1^\alpha p_3^\beta p_2^\rho p_4^\mu.$$

In addition we have:

$$y_1 = 2 \alpha_1 \left[\alpha_1 \alpha_3 (\nu_2 \nu_5 - \nu_1 \nu_4) + 2 \nu_4^2 + \nu_2 \nu_3 \right],$$

$$y_2 = 2 \alpha_2 (\nu_2 \nu_5 - \nu_1 \nu_4) - \nu_2^2 \alpha_1,$$

$$y_3 = - \left(\frac{4 \nu_3}{\nu_2^2} \right) \left\{ \alpha_1 \alpha_3 \left[\nu_1 \nu_2 (\nu_2 + \nu_3) - 2 \nu_4 (\nu_1 \nu_4 - \nu_2 \nu_5) \right] + \nu_4 (4 \nu_4^2 - \nu_2^2) \right\};$$

$$z_1 = \nu_2 \nu_4 \alpha_1^2 \alpha_3,$$

$$z_2 = \nu_2 \nu_4 \alpha_2,$$

$$z_3 = \frac{1}{4} \alpha_1 \left[2 \nu_2 (2 \alpha_2 + \nu_2 + \nu_3) + 4 \nu_4^2 - \nu_2^2 \right],$$

$$z_4 = \frac{1}{4} \alpha_1 \left[4 \nu_4^2 - \nu_2^2 - 2 \nu_2 \nu_3 \right],$$

$$z_5 = - \alpha_1 \alpha_3 \nu_3 (4 \nu_4^2 - \nu_2^2) / \nu_2,$$

$$z_6 = - (\nu_3 \nu_4 / \nu_2) \left[2 \alpha_2 + (4 \nu_4^2 - \nu_2^2) / \nu_2 \right].$$

26.

The σ 's are given explicitly as follows:

$$\sigma_1 = \frac{\alpha_3}{\sqrt{2}} (2\alpha_1^2 \alpha_3 - \nu_2) \xi,$$

$$\sigma_2 = 2\alpha_1 \alpha_3 \nu_2 (\nu_3 + \alpha_1^2 \alpha_3 + \frac{2\nu_4^2}{\nu_2}),$$

$$\sigma_3 = \frac{\nu_1}{\nu_2} (\nu_2 + \nu_3),$$

$$\sigma_4 = 2 \frac{\alpha_3}{\nu_2} (\alpha_2 + \nu_3 + \frac{2\nu_4^2}{\nu_2}) \xi,$$

$$\sigma_5 = \alpha_1 \alpha_3 \nu_2 (2\alpha_2 - \nu_2),$$

$$\sigma_6 = \left[\sigma_7 + \frac{4}{\nu_2^2} \alpha_1 \alpha_3 (\nu_2 \nu_5 - \nu_1 \nu_4) \right] \xi,$$

$$\sigma_7 = 1 + \frac{2\nu_3^2}{\nu_2^2} + \frac{4\nu_4^2}{\nu_2^2},$$

$$\sigma_8 = \left[\sigma_7 + \frac{4\alpha_1^2 \alpha_3}{\nu_2} \right] \xi,$$

$$\sigma_9 = 4\nu_3 \nu_4 \alpha_3 \left[1 - \frac{4\nu_4^2}{\nu_2^2} - \frac{2\alpha_1^2 \alpha_3}{\nu_2} \right],$$

$$\sigma_{10} = \frac{4\nu_3 \alpha_3}{\nu_2^2} \left[\frac{2\nu_4}{\nu_2} (\nu_2 \nu_5 - \nu_1 \nu_4) + \nu_1 (\nu_2 + \nu_3) \right] \xi,$$

$$\sigma_{11} = 1 + \frac{2\nu_3^2}{\nu_2^2} - \frac{4\nu_4^2}{\nu_2^2},$$

$$\sigma_{12} = \frac{4\nu_3 \alpha_3}{\nu_2^3} (\nu_2 + \nu_3) \left(1 - \frac{4\nu_4^2}{\nu_2^2} + \frac{2\alpha_1 \alpha_3 \nu_1 \nu_4}{\nu_2^2} \right) \xi,$$

$$\sigma_{13} = \frac{8\nu_3 \nu_4}{\nu_2^3} \alpha_1 \alpha_3^2 \xi, \quad \sigma_{14} = \sigma_3 \sigma_8 - \frac{8\alpha_1 \nu_4}{\nu_2^3} (\nu_2 + \nu_3) \xi.$$

REFERENCES -

- (1) - See "A review of Recent work in Experimental Quantum Electrodynamics" by R. Weinstein. 1967 International Symposium on Electron and Proton Interactions at High Energies, Stanford Linear Accelerator Center, Stanford, California (1967); D. Quinn and D. Ritson Phys. Rev. Letters 20, 890 (1968).
- (2) - J. A. McClure and S. D. Drell, Nuovo Cimento 37, 1638 (1965).
- (3) - J. Bjorken, S. Drell and S. Frautschi, Phys. Rev. 112, 1409 (1958).
- (4) - R. A. Berg and C. N. Lindner, Phys. Rev. 112, 2072 (1958); P. S. Isaev and I. S. Zlatev, Nuclear Phys. 16, 608 (1960); A. Costescu and T. Vescan, Nuovo Cimento 48, 1041 (1967).
- (5) - R. A. Berg and C. N. Lindner, Nuclear Phys. 26, 259 (1961).
- (6) - M. Greco, A. Tenore and A. Verganelakis, Phys. Letters, (to be published).
- (7) - J. Bjorken and S. Drell, Relativistic Quantum Mechanics (McGraw-Hill Book Company, Inc., New York, 1964).
- (8) - A. P. Contogouris and A. Verganelakis, Phys. Rev. 6, 103 (1963).
- (9) - A. C. Hearn and E. Leader, Phys. Rev. 126, 789 (1962).
- (10) - F. E. Low, Phys. Rev. 96, 1428 (1954); M. Gell-Mann and M. L. Goldberger, Phys. Rev. 96, 1433 (1954).
- (11) - A. Verganelakis and D. Zwanziger, Nuovo Cimento 39, 613 (1965).
- (12) - M. Gourdin and Ph. Salin, Nuovo Cimento 27, 309 (1963).
- (13) - A. J. Dufner and Y. S. Tsai, Phys. Rev. 168, 1801 (1968).
- (14) - R. F. Stiening, E. Loh and M. Deutsch, Phys. Rev. Letters 10, 536 (1963).
- (15) - J. Mathews, Phys. Rev. 137, B 444 (1965); J. D. Bjorken and J. D. Walecka, Ann. Phys. 38, 35 (1966).
- (16) - R. H. Dalitz and D. G. Sutherland, Phys. Rev. 146, 1180 (1966).
- (17) - This quantity has been measured recently in two kinematical configurations by a Frascati - Napoli - Roma group at Frascati (to be published).
- (18) - S. D. Drell, Proc. XIII Intern. Conf. on High-Energy Physics Berkeley, 1966.
- (19) - The main experimental difficulty which arises in the WAB experiments is the problem of how to discriminate the γ 's of the WAB from the γ 's due to the decay of the electroproduced π^0 .
- (20) - A. S. Krass, Phys. Rev. 138, B 1268 (1965); S. D. Drell in Proc. Intern. Symp. on Electron and Proton Interactions at High Energies, Hamburg, 1965 (Springer-Verlag, Berlin 1966) Vol. I, p. 71; J. Asbury, U. Becker, W. Bertran, P. Joos, M. Rohde, A. J. S. Smith, C. Jordan and S. C. C. Ting, Phys. Rev. Letters 19, 869 (1967); R. G. Parsons and R. Weinstein, Phys. Rev. Letters 20, 1314 (1968).
- (21) - H. D. Schulz and G. Lutz, Phys. Rev. 167, 1280 (1968).

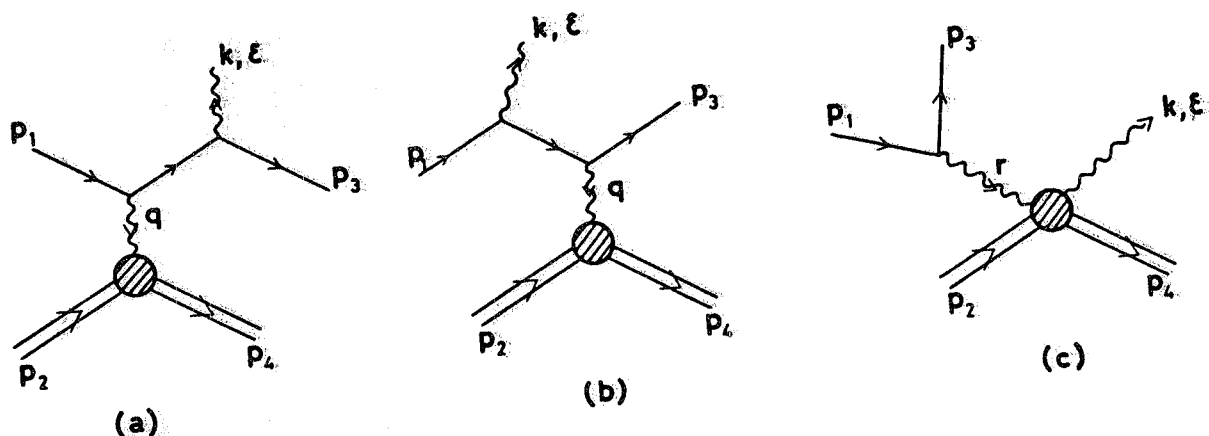


FIG. 1 - First order Feynman Diagrams for wide-angle bremsstrahlung. (a), (b) electron bremsstrahlung;
(c) proton bremsstrahlung.

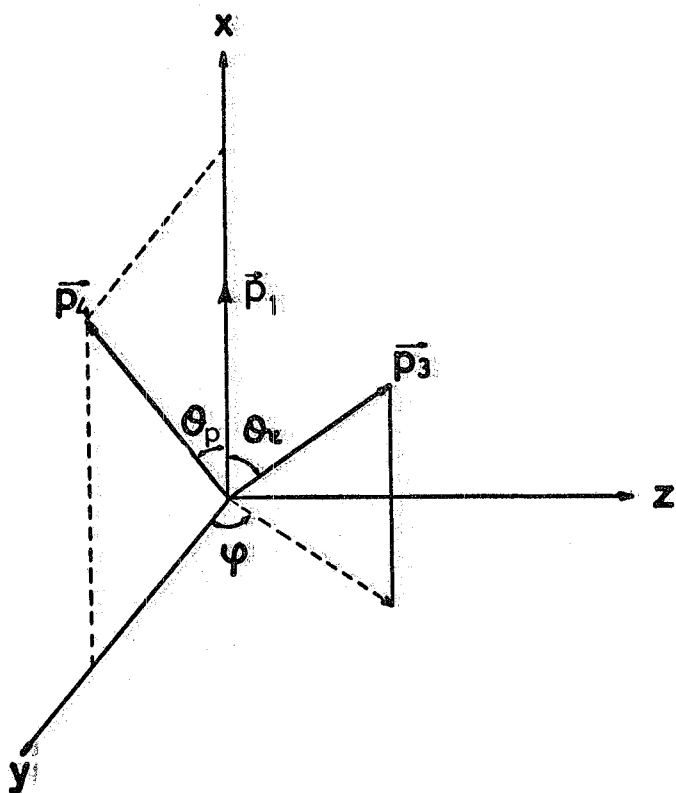


FIG. 4 - Frame of reference used to calculate the tables II and III.

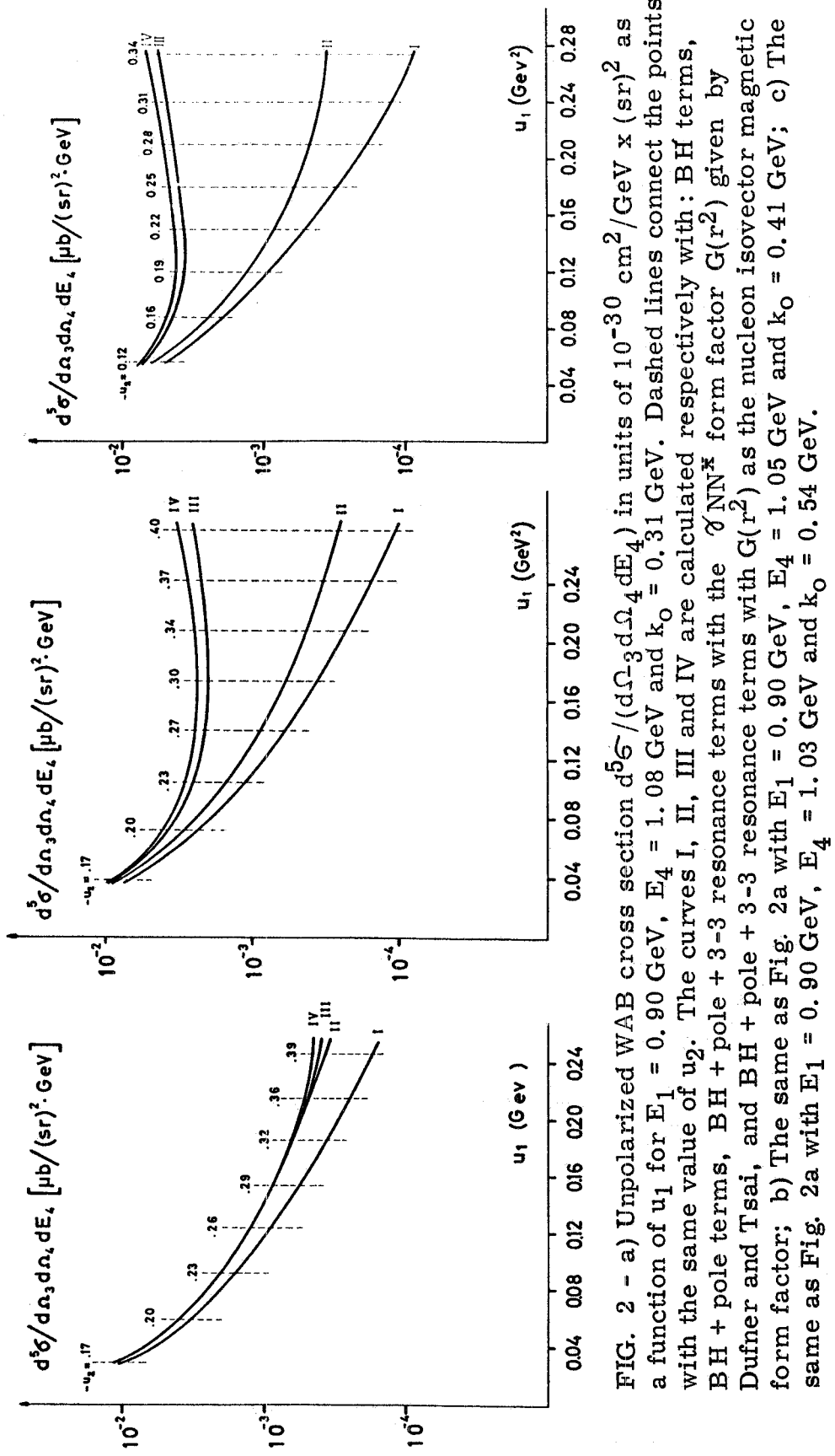


FIG. 2 - a) Unpolarized WAB cross section $d^5\sigma/(d\Omega_3 d\Omega_4 dE_4)$ in units of $10^{-30} \text{ cm}^2/\text{GeV} \times (\text{sr})^2$ as a function of u_1 for $E_1 = 0.90 \text{ GeV}$, $E_4 = 1.08 \text{ GeV}$ and $k_o = 0.31 \text{ GeV}$. Dashed lines connect the points with the same value of u_2 . The curves I, II, III and IV are calculated respectively with: BH terms, BH + pole terms, BH + pole + 3-3 resonance terms with the γ_{NN}^X form factor $G(r^2)$ given by Dufner and Tsai, and BH + pole + 3-3 resonance terms with $G(r^2)$ as the nucleon isovector magnetic form factor; b) The same as Fig. 2a with $E_1 = 0.90 \text{ GeV}$, $E_4 = 1.05 \text{ GeV}$ and $k_o = 0.41 \text{ GeV}$; c) The same as Fig. 2a with $E_1 = 0.90 \text{ GeV}$, $E_4 = 1.03 \text{ GeV}$ and $k_o = 0.54 \text{ GeV}$.

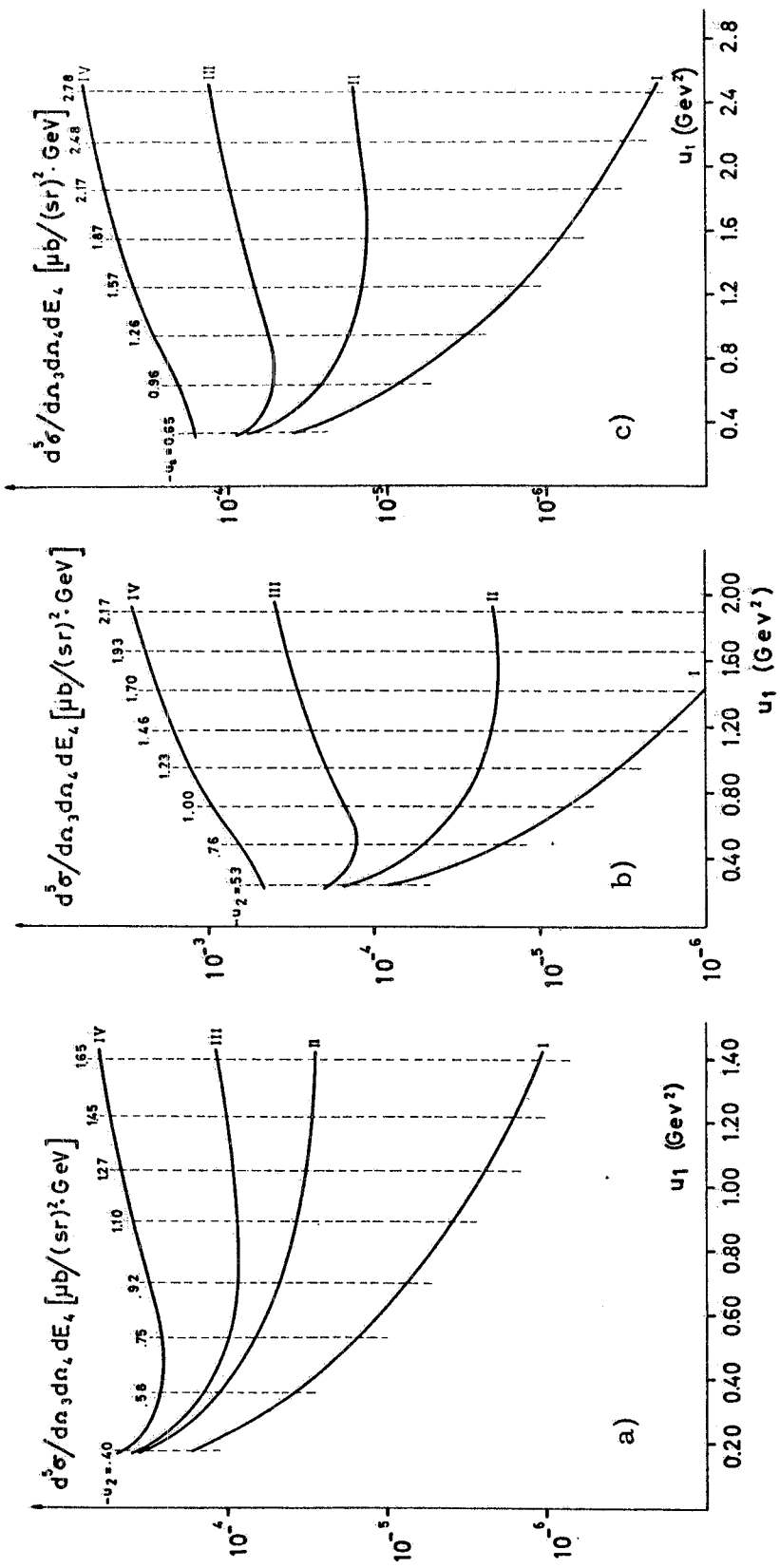


FIG. 3 - a) The same as Fig. 2a with $E_1 = 5.0$ GeV, $E_4 = 3.04$ GeV and $k_0 = 0.35$ GeV; b) The same as Fig. 2a with $E_1 = 5.0$ GeV, $E_4 = 2.92$ GeV and $k_0 = 0.49$ GeV; c) The same as Fig. 2a with $E_1 = 5.0$ GeV, $E_4 = 2.84$ GeV and $k_0 = 0.7$ GeV.

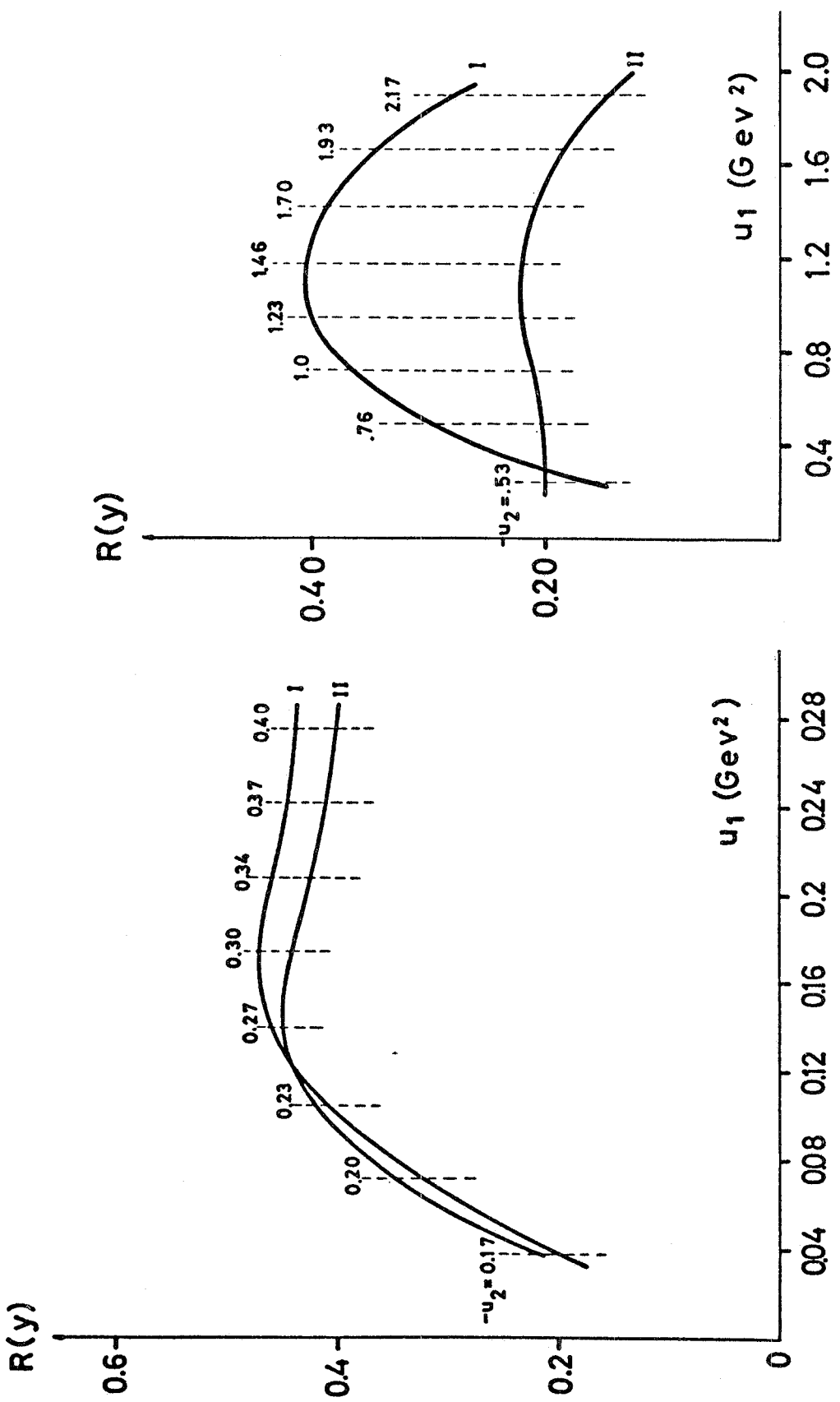


FIG. 5 - a) $R(y)$ defined in the text, as a function of u_1 , for $E_1 = 0.90 \text{ GeV}$, $E_4 = 1.05 \text{ GeV}$ and $k_0 = 0.41 \text{ GeV}$. Dashed lines connect the points with the same value of u_2 . The curves I and II are calculated respectively with $\mathcal{T}_{\text{NN}}^*$ form factor $G(r^2)$ given by Dufner and Tsai, and with $G(r^2)$ as the nuclear isovector magnetic form factor; b) The same as Fig. 5a with $E_1 = 5.0 \text{ GeV}$, $E_4 = 2.92 \text{ GeV}$ and $k_0 = 0.49 \text{ GeV}$.

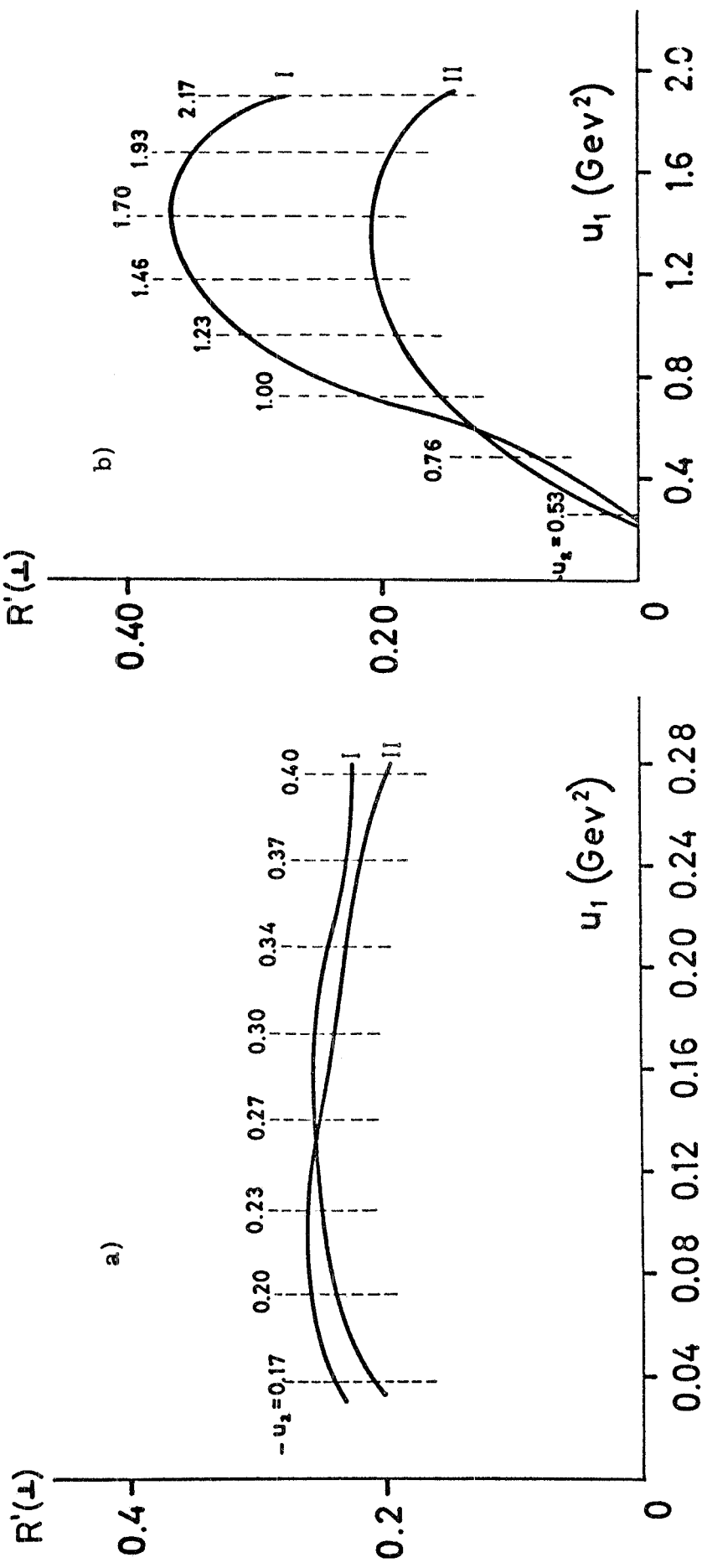


FIG. 6 - a) $R'(\perp)$, defined in the text, in the same kinematical configuration as Fig. 5a; b) $R'(\perp)$, defined in the text, in the same kinematical configuration as Fig. 5b.